We are IntechOpen, the world's leading publisher of Open Access books Built by scientists, for scientists

4,800
Open access books available

122,000
International authors and editors

135M
Downloads

Our authors are among the

154
Countries delivered to

TOP 1%
most cited scientists

12.2%
Contributors from top 500 universities

WEB OF SCIENCE™

Selection of our books indexed in the Book Citation Index in Web of Science™ Core Collection (BKCI)

Interested in publishing with us?
Contact book.department@intechopen.com

Numbers displayed above are based on latest data collected.
For more information visit www.intechopen.com

Chapter 7

Linking Non-equilibrium Transport with the Many Particle Fermi Sea in the Quantum Hall Regime

Josef Oswald

Additional information is available at the end of the chapter

http://dx.doi.org/10.5772/62926

Abstract

The communication of the electron system with the outside world at low excitation transport experiments happens by exchanging electrons at the Fermi level. We argue that the locations where this is possible in the quantum Hall effect regime are the so-called edge channels. We explain that these channels can be understood as a more general representation of the many-particle quantum Hall (QH) system close to equilibrium that allows describing transport due to non-equilibrium on a very fundamental level. Based on fundamental principles of quantum physics, a transfer matrix formulation for the local non-equilibrium electrochemical potential in a network of interconnected directed quantum channels can be used to solve the lateral distribution of the non-equilibrium excitation potentials. Instead of using the Landauer formula or other tools like the Kubo formula for addressing conductance's just a transfer matrix formulation for the transfer of electrochemical potentials is used to find the self-consistent lateral distribution of the non-equilibrium electrochemical potentials. Currents and potentials that are measured at contacts are only calculated as a post-processing step right at the contacts, and they allow calculating all the resistances and conductance's like known from QH experiments. The interplay between transport and the many-particle system is of general interest when dealing with accessing information about quantum systems. Our approach allows modeling electron systems in the QH regime for realistic sample geometries, including inhomogeneities, like present in real samples or that are forced by gate electrodes as well as the random disorder potential. We combine our network model for transport with the Hartree–Fock method that allows the inclusion of realistic screening effects as well as the magnetic field-dependent enhanced g-factor.

Keywords: network model, quantum Hall effect, magneto-transport, conductance quantization, non-equilibrium transport, exchange interaction, Hartree-Fock approximation, many particle quantum system

1. Introduction

Even more than 35 years after discovering the integer quantum Hall effect [1], it is still a lively discussed topic at many conferences. In the quantum Hall (QH) regime, the many-particle quantum nature of the electron system can be studied from mesoscopic to nearly macroscopic length scales. The challenge in modeling electron transport in this regime is that the many-particle quantum states of the electron system exist as stationary states at thermal equilibrium, while transport is driven by introducing deviations from the equilibrium. Even for the QH experiments that happen close to thermal equilibrium, a direct modeling of current flow does not fit the world of stationary states. The general purpose of quantum Hall effect experiments is to unveil the physics of the stationary many-particle quantum states behind. This implies that such experiments should happen close to the thermal equilibrium and therefore they are mostly performed also at lowest achievable temperatures. However, any experiment in quantum physics is a disruption of the quantum states under investigation and that is true also for the quantum Hall experiments. On this background, the major question arises to what extend experiments can provide information about the underlying physics of the stationary many-particle states. At the same time, one has to consider that the stationary state under investigation itself cannot be directly used for modeling current flow. Stationary states do not exhibit any time-dependent observables, except while destroying them. This fundamental dilemma can be seen as the playground for the numerous theoretical approaches to the quantum Hall effects in order to compare theory and experiment. Various theoretical approaches focus on finding a basis for relating steady state properties of the quantum system to experimental properties without finally being able to model directly the current flow like it happens in the various experiments. One most prominent theoretical approach is the scaling theory [2], that is based on the localization picture of the quantum Hall effect and that relates the localization length of the stationary quantum states to experimental properties like the width of the quantum Hall plateau transition regimes that can be affected by experimental conditions like temperature [3] and measurement frequency [4]. Despite the great success of this theory, that finally proofs the quantum nature of the physics behind; the current flow itself is not addressed by this method. A further step in this direction is the usage of local conductance's that are extracted from the network of quantum channels evolving for the steady state. However, local conductances are finally introduced even for such most successful and sophisticated methods like, for example, the Kubo formula [5], while any local quantities associated with local current flow is finally a violation of the many-particle physics, as will be discussed in the next section.

2. Single-particle picture versus many-particle states

One of the most important aspects for the interpretation and modeling of experimental investigations is the fact that electrical measurements in the quantum Hall regime deal in fact with single particles in terms of counting carriers when measuring currents. On this background, it is not that surprising that also the interpretation and the way of thinking about the quantum Hall system is dominated by the single-electron picture. Anyway the human ability

http://dx.doi.org/10.5772/62926

for thinking, intuition and finally picturing processes that take place in the electron system is limited to the imagination of single electrons, or at least single quasi-particles. From the general point of view, any electrical measurement as performed in the quantum Hall system has to be understood as an extraction and/or injection of single electrons from and to a many-particle quantum system at the contacts, while any imagination of the movement of single electrons between those contacts in the electron system must consequently fail and is finally forbidden. However, there still exist very useful pictures and models that are based on single electrons moving along the quantum Hall systems like, for example, the edge channel picture [6] that has proven to be very successful especially for the interpretation of QH experiments. Last but not least the scientific community needs such restricted pictures in order to communicate and deal with the subject. Therefore, it is a special challenge to find out to what extend such single-electron pictures may be used without seriously violating the many-particle physics behind, but also finding out, why such "wrong" pictures still give right answers and where the limits for the applications of these "wrong pictures" are. In the following, we finally try to extend the limits of these "wrong" single-particle pictures by a modified interpretation of the single-electron picture.

As already mentioned, one of the most prominent and useful single-electron pictures in the QH physics is the so-called edge channel picture that gives useful results even when considering the single electrons as interaction free. Edge channels act as one-dimensional directed quantum channels. However, before having a closer look to this model, we should have to look at some basic aspects about one-dimensional channels in general.

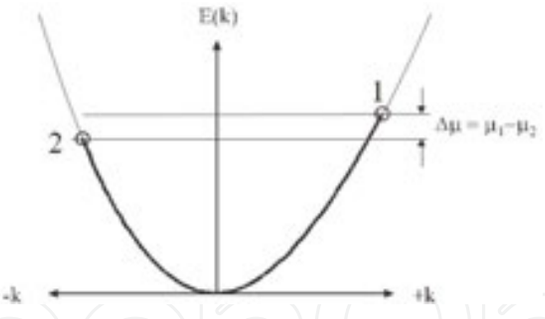

Figure 1. Band structure of a one-dimensional channel with parabolic k-branches for forward and backward direction; labels 1 and 2 indicate the quasi-Fermi levels for the case of an injected non-equilibrium by opposite contacts. The bold parabolic branches indicate the filled states in k-space, which are different for the two k-branches at non-equilibrium.

Figure 1 schematically shows the band structure of a one dimensional channel. It consists of two branches in k-space, one for the forward and one for the backward direction of the channel. This picture is often used to introduce the one-dimensional quantized conductance, and it allows getting the correct value of $G=2^{e^2}/h$ for spin degenerate electron channels on the basis of semiclassical arguments. The main assumption for this is that only those electrons contribute to the current that are occupying states in the energy interval between μ_1 and μ_2. However, despite the correct result, this picture gets in serious conflict with the many-particle nature of the electron system if one takes that assumption for true. Already the interpretation of this

simple picture seems to be crucial, and it is worth to find out why to some extend the main results are still valid and if we need to change the way of thinking how the single electrons in the channel carry the current.

It is well known that according to the above semiclassical model, a net current flows, if the two branches in k-space are driven out of thermal equilibrium by applying different voltages to the contacts that inject carriers from opposite sides via the opposite k-branches. However, a common misinterpretation in this context is now to say that all electrons on opposite lying states in k-space do not produce a net current flow because of k-cancellation; only those electrons occupying the states between μ_1 and μ_2 produce a net current that can be measured in experiments. If thinking this way, we attribute single individual electrons to single quantum states; or at least, we attribute different groups of electrons to sit on different regions in k-space. That is clearly in contradiction with the many-particle picture, because that interpretation suggests that only a small fraction (group) of (necessarily distinguishable) electrons carry the current. According to the many-particle picture, all electrons and single-electron states should lose their individuality and it should not be allowed to attribute any subset of electrons to any subset of states. Nevertheless, the consequent further application of this interpretation leads still to the correct value of the one-dimensional conductance. This fact makes it difficult to realize if the limits of interpretation are already violated or not. We identify this as the main source of many controversial discussions in the community. But how can we think about electrons acting in any system without the ability of attributing subsets of electrons to particular regions, states, or considering different electrons for different actions?

In order to reconsider this problem for trying to find an appropriate re-interpretation, we would like to draw the attention back to the very basics of the many-particle picture. It is well known that the many-particle states are composed by single-particle states by superposition while mixing up all different configurations for the occupation of different states by different electrons. This means that all single electrons lose completely any relation or association with any particular states and they get complete delocalized in space as well as in energy. This happens while preserving the negative Eigenvalue of the operator for exchanging any two single electrons of the system, like demanded for Fermions. Just as a reminder, the composition for a two-electron state in this context reads as follows:

$$|\psi\rangle = \frac{1}{\sqrt{2}}\left\{\left|\psi_1, \psi_2\right\rangle - \left|\psi_2, \psi_1\right\rangle\right\} \tag{1}$$

Here, $|\psi_1, \psi_2\rangle$ means that electron 1 occupies state 1 and electron 2 occupies state 2, while $|\psi_2, \psi_1\rangle$ means electron 1 occupies state 2 and electron 2 occupies state 1. By superposition of the different configurations, the electrons lose their identity and their association with a particular single-electron state and the negative sign in the superposition ensures the required change of sign when interchanging any two electrons as required for Fermions. For more than two electrons and more than two states, this composition is done in real space representation by applying the so-called Slater determinant for mixing up all possibilities of attributing all

http://dx.doi.org/10.5772/62926

electrons to all available single-electron wave functions. This technique is applied also in context with the Hartree–Fock [7] approach as used in our modeling below. At this point, only the fundamental consequences should be brought back to attention. The crucial point is that the human way of thinking is always bound to the imagination of single electrons and the fundamental question arises if there exists a more appropriate way of intuitive thinking about single electrons that is more suitable for the many-particle physics. This question is important, because most of the controversial discussions in the scientific community arise from the way, how different people obtain their mostly intuitive understanding in terms of single electrons, which anyway has to fail at some point for the many-particle system. Therefore, we have to re-interpret the single-electron aspect on the background of the many-particle system. For this purpose, we have to answer two fundamental questions that have to be correctly answered also by any interpretation in terms of single electrons [8]:

I. *What is the ground state energy of the many-particle system?*

II. *Which of the supposed single electrons are sitting right at that ground state energy?*

According to the basic principles of quantum physics, the ground state energy has to be defined in terms of an "observable" that needs an appropriate operator for measuring that physical quantity. This "measurement" has to be based either on a real experiment or at least on a "Gedankenexperiment." On this basis, the two questions can be re-formulated as follows:

ad I) At which energy can we extract any single electron from the system without destroying the ground state of the system left behind, after just taking an electron, or just adding an electron?

It quickly becomes clear that a single electron has to be extracted from or added to the Fermi level if subsequent relaxation processes of the electron system should be avoided. If we, for example, pull out an electron at lower energy than the Fermi energy, an excited hole would have been left behind that subsequently relaxes. If adding an electron at higher energy, it is also clear that we would create an excited state that still has to relax into the ground state subsequently. The only way to put in or take out an electron without the need of subsequent spontaneous relaxation is if that happens right at the Fermi energy. The Fermi energy therefore appears as the lowest possible energy at which the electron system can communicate with the outside world, as, for example, done by a transport experiment at low temperatures and low driving currents. Consequently, the Fermi energy should be defined as the (observable) ground state of the many-particle systems.

ad II) What is the probability for "catching" any particular single electron of the system at the Fermi energy?

We consider the electron system in the ground state as a black box, and we randomly take out and put back electrons at the Fermi level according to I. Knowing how the many-particle state is constructed [see e.g. Eq. (1)], it becomes immediately clear that we can find each individual electron of the system with same probability sitting at any electronic state, which applies of course also for the Fermi level! So if one particular electron out of N electrons can be found at the Fermi level with probability $^{1}/_{N}$, this can only mean that all single electrons sit right at the

Fermi level. In this case, the "observation" has to overrule some possibly contradicting intuition.

In contrast to the most common way to look at the many-particle electron system in a single-electron representation, we consequently have to consider all single electrons sitting right at the Fermi energy.

Except this maybe somehow counter intuitive fact which we have to accept some how, we now can go on to think in terms of single electrons. In this context, it is interesting to reconsider the conductance of the one-dimensional channel according to **Figure 1**: All electrons are considered to sit at the top occupied energy level, that is, twofold degenerate for the +/− k-branches in the case of equilibrium. Additionally, the "single electrons" are also delocalized between these degenerate levels because of the many-particle character of the whole system. The single-particle wave functions are consequently just plane waves at k_F for *all* electrons, which still compensate each other at thermal equilibrium, meaning that the quasi-Fermi levels in the two branches of the k-space are the same (see **Figure 2** left) and the counter-propagating identical electron waves create a stationary periodic charge distribution along the channel.

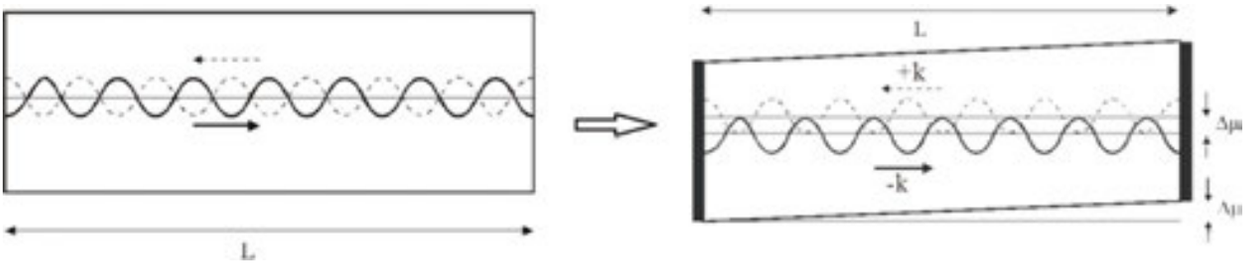

Figure 2. Left: Counter-propagating electron waves from states in the opposite k-branches at Fermi level for equilibrium. Right: Counter-propagating electron waves from states in the opposite k-branches at quasi-Fermi levels that are slightly shifted against each other by a small potential difference introduced by opposite contacts.

If we now introduce a vanishing small non-equilibrium Δμ between the two k-branches by applying a vanishing small potential difference at the associated contacts, the two counter-propagating single-electron wave functions face a slight energy difference that affects the result of their superposition (see **Figure 2** right). This energy difference affects the usually not observable universal time dependence of stationary quantum states that reads as follows:

$$\psi(x,t) = \psi(x) \cdot e^{-i\frac{2\pi \cdot \mathrm{E}}{h}t} \tag{2}$$

However, this time dependence becomes relevant in case of superposition. The superposition of the counter-propagating waves with slightly different energy E_I and E_{II} leads now to a beating effect in time that causes a lateral movement of the whole charge distribution that is associated with the superposition that originally resembles just a standing wave (that now starts to move). The beating frequency ν therefore derives as $\nu = \Delta\mu / h$ which finally leads to a non-stationary time-dependent state that now creates charge transport. This fact can be seen as a most elementary step of composing a non-stationary state by the superposition of two

http://dx.doi.org/10.5772/62926

stationary states at slightly different energy. It is easy to convince oneself that during a single beating cycle, the original charge distribution is restored, while the charge distribution as a whole moved on by exactly one period of the initial charge distribution. This represents a certain transferred charge from one contact to the other. We know that a single electron on the Nth quantum state in space representation is build up by N charge maxima that are distributed along the channel. Since they shift laterally by one period during a single beating cycle, the transferred charge relates to a fraction of $\Delta q = q_e/\mathrm{N}$ of the charge of one single electron. However, due to the many-particle aspect and the Pauli principle, we know that we have also a total of N electrons in the whole system that subsequently fills up all lower states. Since we have to consider all N electrons equally at the Fermi energy, they consequently contribute all equally in parallel. All together we get therefore a charge transfer of N times the fraction Δq of charge. This gives in total charge per beating cycle of $\Delta Q = N \cdot \Delta q$. This finally appears to be the charge of a single electron q_e. As a consequence, we obtain the fundamental result that the complete electron system transfers exactly the charge of one single electron during each beating cycle from one contact to the other. Assuming spin degeneracy, we just have to multiply by a factor of 2 and we get $I = 2 \cdot \nu \cdot q_e$ as the total current which easily allows deriving an associated conductance:

$$G = 2 \cdot \frac{e^2}{h} \tag{3}$$

In this way, we end up with the well-known quantized value for the conductance of a spin degenerate one-dimensional channel. However, it results from a slightly different way to look at the many-particle systems in term of single electrons that strictly avoids attributing individual electrons to individual single-electron states, but at the same time including all electrons of the system.

If we reconsider now the implications for transport experiments, it becomes clear, that for low-excitation experiments close to the thermal equilibrium, the electron system is only accessible in regions where the spectrum of the single electrons has states close to the Fermi level. These Fermi edge electrons take the role as a representation of the whole electron system that, however, can be accessed close to the ground state only at the Fermi level. Therefore, these electrons seem to appear just at locations, where there are states at the Fermi level in the single-electron picture that make up the quantum channels or so-called edge channels in the QH regime. However, it is a common misinterpretation to conclude that current carrying electrons exist only in those channels. Moreover, according to the composition of the many-particle states, it is even forbidden to attribute single electrons to special regions, energies, and states. The channels are only regions where one can communicate with the electron system close to thermal equilibrium, while the electrons themselves remaining de-localized over the whole system [8]. We may picture the transport channels as the dip of the iceberg that sticks out of the Fermi sea, but still belonging to the one and only many-particle system. Doing low-excitation transport is like walking on the tip of the iceberg, and it crucially depends on the topology of the ground on the dip.

The consequences of these considerations in this paragraph will become clearer if applying them to the edge channel picture in the next paragraph.

3. The edge channel picture

Since the edge channel picture [6] is a widely known model, only a short qualitative overview of the main aspects should be given in this chapter. However, we need this chapter in order to make clear the consequences of the above discussion and the implications for our modeling below. The main ingredient of how edge channels are created is that for the Schrödinger's equation a strong homogeneous magnetic field appears as an effective parabolic confinement potential that acts in addition to a possibly present electrical potential. A strong magnetic field in this context is present, if the magnetic length is small as compared to the typical length scales of the electrical potential or in other words, if the electrical potential varies slowly on the length scale of the cyclotron radius. However, the centre coordinate for the magnetic contribution to the confinement potential is not fixed in space and has therefore a free centre coordinate for the Schrödinger's equation (see e.g. Ref. [9]). Furthermore, for realistic magnetic fields of several Tesla and sample parameters as used in real experiments, the quantization due to the magnetic confinement dominates strongly over the contribution of the electrical field. In this regime, the quantization due to the magnetic field leads to the well-known Landau levels, just like without electrical field. It appears as a good approximation for the energy spectrum that the local electrical potential simply shifts the magnetically split LLs parallel in energy. This is shown in **Figure 3**.

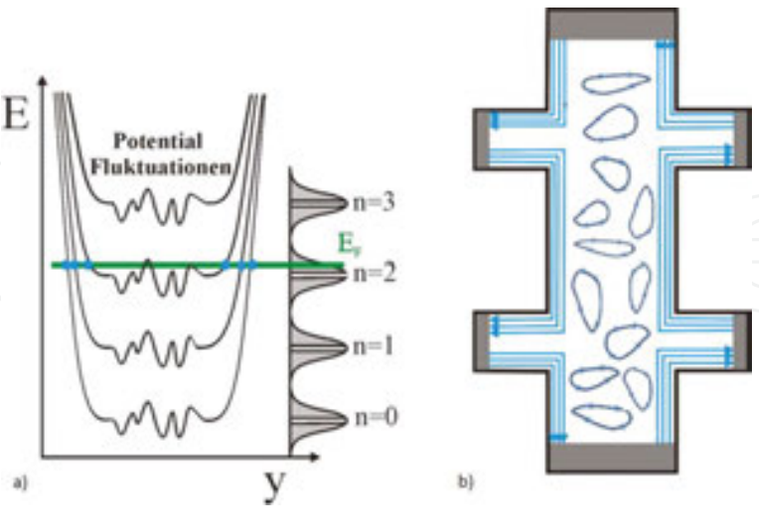

Figure 3. (a) Schematic representation of the laterally varying Landau levels across the bulk in the transverse y-direction that mimic the lateral electrical potential fluctuations; at interceptions with the Fermi energy, there appear directed channels that resemble loops around potential hills or valleys and edge channels along the sample edge near the sample boundaries (blue color); (b) schematic representation of the Hall geometry with the bulk area in top view with the edge channels along the edge and loops (magnetic bound states) in the bulk region.

http://dx.doi.org/10.5772/62926

In this regime, the states at the Fermi energy (E_F) extend only along equipotentials, where the LLs intercept E_F, while in direction transverse to the equipotentials, they are localized on the length scale of the cyclotron radius. These equipotentials resemble directed channels along the edges of the electronic system and create directed loops in the bulk region that might also couple opposite edges by tunneling across magnetic bound states [10]. Conduction through the bulk becomes possible, if the bulk states, that mostly create localized loops, extend over the sample size. That happens, if the Fermi level is close to the centre of the potential fluctuations, which also means the centre of the disorder broadened LL. Whenever a bulk current is possible, we get into the regime between QHE plateaus and whenever the bulk is insulating, we are in the plateau regime. This aspect is used by the Chalker–Coddington network model [11], which has been introduced in order to calculate the localization length that is decisive for the bulk states whether they contribute to the spectrum of the localized states or they belong to the spectrum of de-localized states within the DOS peaks of the LLs.

Figure 4 schematically summarizes the results of the so-called localization picture of the QHE [12] that finally leads to the scaling theory of the QHE [2]. The essential point of the scaling theory is that the localization length of an electronic state close to the centre of the Landau level scales according to a particular exponent of the inverse energy relative to the LL centre.

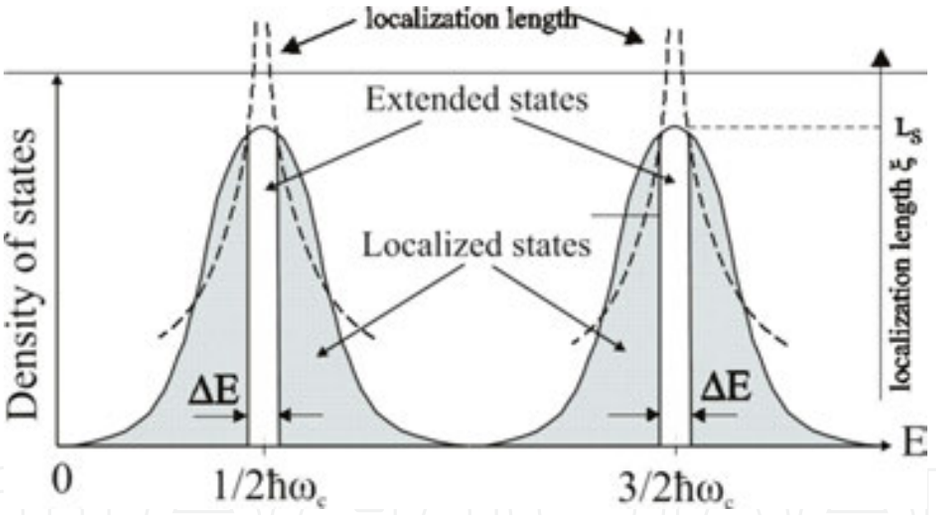

Figure 4. Schematic representation of the localization picture of the integer quantum Hall effect. It illustrates the density of states (DOS) for the two lowest Landau levels (LL). The energy interval ΔE indicates that part of the DOS around the centre of the LL, in which there exist delocalized states with respect of the sample size. The shaded tails of the DOS are explained to contain localized states. The dashed lines indicate schematically the dependence of the localization length ξ on the energy of the states relative to the LL centre.

This suggests that at zero temperature the localization length would diverge to infinity for one particular energy right at the centre of the LL. For finite sample size, any localization length larger than the sample size produces consequently delocalized states that open up a window of de-localized states around the LL centre. But also a finite temperature opens up such a window because a finite temperature brings in a phase uncertainty that destroys quantum-driven localization mechanisms like, for example, Anderson localization for localization

lengths above certain values. Intensive experimental investigations of this scaling behavior as well as theoretical investigations confirmed that the scaling exponent results from quantum percolation, which can be seen as the main message for the ongoing chapter.

In conclusion of the scaling theory, the experimentally obtained scaling exponent suggests that bulk transport is indeed driven by quantum percolation. We also want to emphasize at this point that the Chalker–Coddington network model is a powerful tool for successfully dealing with the localization problem, but definitely it deals with the stationary states of the system at the Fermi level at equilibrium. The mapping onto the scaling behavior of experimentally investigated quantities is the most important contribution of the CC model for understanding the QHE, but it does not directly explain the excess current flow as it happens in real experiments.

4. Introducing non-equilibrium

From the previous section, we conclude that the channels of non-vanishing DOS at the Fermi level which develop at the intersections of the LLs with the Fermi energy are indeed quantum channels. Now, we need a model that captures the behavior of these channels if introducing non-equilibrium like in real experiments.

In **Figure 3**, there has been already shown a QHE sample with edge channels, as introduced by Büttiker [6]. The blue lines are the edge channels that appear as intersections of the LLs that follow the uprising potential at the edges of the sample. Topologically opposite pairs of channels belong to a single channel that follows the edge all around the sample. However, current contacts at the ends break up the loop, leaving two opposite directed channels, but they have still to be understood as parts of one common channel (still created by one and the same many-particle electron system). These opposite directed channels can be seen as the two opposite branches in k-space of an ordinary one-dimensional channel as depicted in Section 2. From this point of view, such a pair of opposite located edge channels have still to be understood as one single one-dimensional channel that in total is able to contribute the quantized conductance. The most important criterion is that one must not consider the edge currents as real currents located just at the edges while current flowing just in narrow channels. Using the arguments given in Section 2, the edge channels are not more than the locations on the sample area, at which one can communicate with the electron system close to equilibrium by transport experiments (the channels are the possible walk ways on the dip of the "many-particle iceberg"). But it is not allowed by quantum physics to even think that single electrons are moving just there semiclassically like in a narrow classical conductor. In other words, the so-called edge current is not a current flowing at the edges; it is carried by the edge channel pair as a whole that is just a representation of the whole electron system. According to the many-particle character of the whole electron system, all electrons are delocalized in between, which means that the path for single electron is completely unknown between the sample boundaries, as it should be in a quantized system. On this background, the historic battle between the so-called edge channel picture and bulk-current picture of the QHE has no real

http://dx.doi.org/10.5772/62926

meaning and is just a result of overstretching the single-electron picture as discussed in Section 2.

If we look at the bulk region, the interceptions with the Fermi energy produce mostly closed loops around hills or valleys of the potential fluctuations which would encircle those in opposite directions. Physically, those loops are the same like the edge channels which run all around the sample, except that edge channels will be interrupted by contacts, while in the bulk region these channels stay to be closed loops. The only way to connect to those loops is either by tunneling if such loops come close to each other at potential saddles, or if such loops finally start to merge, while the Fermi level touches the saddle energy.

The plateau regime of the quantum Hall effect is perfectly described by the edge channel picture that in this context means indeed the channels that run along the edge, while the bulk channels do not contribute. However, the physically most interesting and challenging problem is the transition regime between QH plateaus, at which also a bulk current is flowing. The representation of this bulk current is therefore is the major goal of the ongoing discussion.

A fundamental building block of our approach is the tunneling regime between loops at the potential saddles. Such saddles exist in real electronic structures in a random potential, but as will be shown subsequently they can be used also as the nodes or building blocks of a network approach in order to discriticize a realistic random potential distribution.

For this purpose, we represent such a saddle by some kind of circuit element that consists of two counter-propagating channels that get close to each other and couple, for example, by tunneling.

Figure 5 shows the situation of two counter-propagating channels, while they get close at the potential saddle and can couple by tunneling. The channels are part of closed loops that can couple also at other saddles to other loops as will be shown below. The most important aspect now is how a tunneling current between the channels has to be handled. In this context, our discussion in Sections 2 and 3 play a major role. There we argued that the counter-propagating channels can be seen as those regions, at which transport close to thermal equilibrium is possible, but all channels belong to the same many-particle quantum state as a whole. If we forget about the association with particular channel pairs unlike done in **Figure 5**, we get two possibilities for building channel pairs, as would be the case if considering the encircled node as a black box. The one is like shown in **Figure 5**, but there is also the possibility to build a pairs with channels 1 → 4 and 3 → 2. Considering the saddle as black box both combinations are possible on equal basis and therefore have to be just different representations of the same problem. If we now consider an introduced non-equilibrium at input channels 1 and 3 that means that the input potentials V_1 and V_3 are set to be different, the associated currents have to serve consistently both possibilities to build channel pairs. Using channel pair 1 → 2 and 3 → 4, they represent a horizontal current transport in **Figure 5** from the right to the left by $I_{xx}=(\mu_1-\mu_4)\cdot {}^{e}\!/\!_{h}$ that is also $I_{xx}=(\mu_2-\mu_3)\cdot {}^{e}\!/\!_{h}$. Using the notation for the quantum Hall effect I_{xx} would serve as sample current, $(\mu_1-\mu_4)$ and $(\mu_2-\mu_3)$ would be measured like Hall voltages, while $(\mu_1-\mu_2)$ and $(\mu_4-\mu_3)$ would be measured like longitudinal voltage drops. However, considering 1 → 4 and 3 → 2 as channel pairs, they represent a current in vertical direction

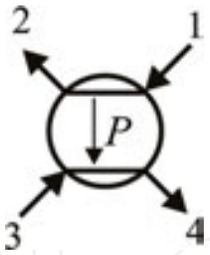

Figure 5. Representation of the situation at a saddle point that can be used as a node of a network. The channels 1 → 2 and 3 → 4 pass each other and the tunneling rate between them is represented by the factor $P = R/T$ where R means the tunneling probability and $T = 1 - R$.

$I_{yy} = (\mu_1 - \mu_2) \cdot {}^{e}/_{h}$ that is also $I_{yy} = (\mu_3 - \mu_4) \cdot {}^{e}/_{h}$. For the quantum Hall notation, in this case, I_{yy} would serve as sample current, $(\mu_1 - \mu_2)$ and $(\mu_4 - \mu_3)$ would be measured like Hall voltages, while $(\mu_1 - \mu_4)$ and $(\mu_2 - \mu_3)$ would be measured like longitudinal voltage drops. In this context, we can interpret the saddle situation in **Figure 5** as a single-channel quantum Hall sample, for which we define the longitudinal voltage drop in horizontal direction as $V_{xx} = V_1 - V_2$ that is also given by $V_{xx} = V_4 - V_3$ and the Hall voltage $V_{xy} = V_1 - V_4$ that is also given by $V_{xy} = V_2 - V_3$. Using further the definition of the longitudinal resistance $R_{xx} = {}^{V_{xx}}/_{I_{xx}}$ and the Hall resistances $R_{xy} = {}^{V_{xy}}/_{I_{xx}}$, we can write the following equations:

$$R_{xx} = \frac{R}{T} \cdot \frac{h}{e^2} \tag{4}$$

$$R_{xy} = \frac{h}{e^2} \tag{5}$$

The above equations use also the fact that the relation between the currents ${}^{I_{yy}}/_{I_{xx}}$ is identical to the associated relation between the probabilities for single carriers that means ${}^{I_{yy}}/_{I_{xx}} = {}^{R}/_{T}$ and we define $P = {}^{R}/_{T}$. There is another interesting fact to be checked: A current I_{xx} and a longitudinal voltage V_{xx} imply a dissipated power of $P_{xx} = I_{xx} \cdot V_{xx}$ in the node. However, since a particular choice of the channel pairs is just one of two possible equivalent choices for the same electron system, the other choice of tunneling current I_{yy} and transverse (Hall) voltage V_{xy} with dissipated power $P_{yy} = I_{yy} \cdot V_{xy}$ should represent the same power dissipation $P_{yy} = P_{xx}$, which is indeed the case and can be easily checked. Turning the node by 90°, which means flipping the x and y directions leads just to a replacement of P by ${}^{1}/_{P}$. The most important aspect is that we can use this node as a kind of building block to build a more complex circuit as a network. Also in real, it happens that several loops get arranged in the bulk region of a real sample that

http://dx.doi.org/10.5772/62926

may get interconnected by tunneling. Therefore, as the next step we use a periodic arrangement in two directions to fill the space in two dimensions. This is schematically shown in **Figure 6** below.

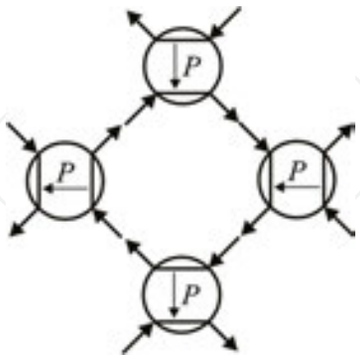

Figure 6. Arrangement of the nodes in Figure 5 in order to resemble a single closed loop in the bulk that allows coupling to adjacent loops in order to fill up the whole area.

From **Figure 6**, one can easily imagine that it is possible to fill up the space with any number of adjacent loops that may fill the bulk region. However, besides the Eqs. (4) and (5), we need a more compact relation that allows obtaining the output potentials of the nodes in terms of the input potentials. For this purpose, we rewrite Eqs. (4) and (5) in terms of potential differences, which means $(\mu_1-\mu_2)=(\mu_4-\mu_3)=\left(R/T\right)\cdot(\mu_1-\mu_4)=\left(R/T\right)\cdot(\mu_2-\mu_3)$. After some steps of derivations, we can show that for each single node, the potentials of the input channels are translated to the potentials of the output channels by some kind of transfer matrix:

$$\begin{pmatrix}\mu_2\\ \mu_4\end{pmatrix}=\begin{pmatrix}T & R\\ R & T\end{pmatrix}\cdot\begin{pmatrix}\mu_1\\ \mu_3\end{pmatrix} \tag{6}$$

This provides a basis for a numerical approach to find the lateral distribution of the potentials over the whole network. It should be emphasized at this point that these are potentials that have to be understood as the deviations from the equilibrium potentials that would be all the same in thermal equilibrium, which of course is the trivial solution for the network. For a non-trivial solution, we need at least two channels of the whole network to be fixed at different potentials, so that the remaining network has to adjust self consistently to these non-equilibrium potentials.

Considering the single nodes of the network, the tunneling current between adjacent loops depends on the relative position of the Fermi energy and the saddle energy, while the smoothness of the saddle potential serves an important parameter. However, this also means that a formulation in terms of the filling factor should be possible too. In Ref. [13], this problem has been considered in detail and formulations have been presented for the dependence on the Fermi energy as well as the dependence on the filling factor. The main results will be discussed in the following and for details please refer to the cited literature [13].

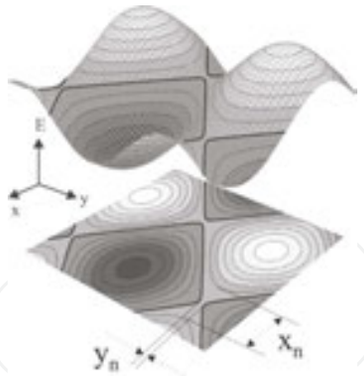

Figure 7. Saddle potential that is produced by a two-dimensional Cosine function; x_n and y_n are the tunneling distance between loops, if they come close to each other in either x or y direction.

As a first step, the situations have been analyzed for saddle potentials that are created by a two-dimensional Cosine function. However, the choice of this special function is not a restriction to a special case, because tunneling becomes important only if the Fermi level gets close to the saddle energy at which the opposite channel can get close to each other. In this regime, the saddle potential can be represented already in very good approximation by the second-order saddle curvature, which is very well parametrized by a Cosine function in both directions. **Figure 7** shows a part of the potential modulation near such a saddle. The bold line for this case represents the channels at a Fermi energy that is slightly below the saddle energy, at which the loops encircle the potential valleys and get close to each other in y-direction by y_n. If the Fermi level moves slightly above that saddle energy, it is easily seen that the loops will encircle potential hills in opposite direction and they get close to each other in x direction by x_n, which resembles a node that is turned by 90°. On this basis, the following equation has been found in Ref. [13]:

$$P = exp\left[\pm\frac{L^2 E_F}{e \cdot V_0} \cdot \frac{e \cdot B}{h}\right] \tag{7}$$

In this equation, E_F is the Fermi energy relative to the saddle energy, L is the period, and V_0 is the amplitude of the representing Cosine function that has been taken into account up to the second-order Taylor expansion. If the Fermi energy crosses the saddle energy, the argument of the exponent changes sign which automatically means that $P \rightarrow {}^{1}\!/_{P}$ and at the same time, the node turns by 90°, as already mentioned above. Considering one square of length L, that is, one full period L of the Cosine function in both directions, the above equation can be mapped onto the filling factor scale [13]:

$$P = exp\left[-\Delta\nu \cdot L^2 \cdot \frac{e \cdot B}{h}\right] \tag{8}$$

http://dx.doi.org/10.5772/62926

$\Delta\nu$ is the difference of the filling factor relative half filling. The above equation suggests that at half filling at $\Delta\nu = 0$ exactly half of the area defined by L^2 is occupied with electrons.

As can be seen in **Figure 8b**, at exactly half filling when the Fermi level meets the saddle energy, exactly half of the area appears as shaded, which means filled with electrons. If the Fermi level is slightly above the saddle like shown in **Figure 8a**, a small shaded gap opens right at the saddle that indicates that the shaded area starts to dominate, and at the same time, the shaded areas get interconnected to each other across the saddle, while the unshaded areas shrink to isolated droplets. The opposite happens if the Fermi level is slightly below the saddle energy like shown in **Figure 8c**, because in this case, a gap of empty states now opens up at the saddle that now interconnects the unshaded areas and leaving the shaded areas as isolated droplets. This behavior is in agreement with the so-called bulk-current picture of the QHE regime that is explained as a mixture of a so call QH liquid phase (shaded area) and an insulating phase (unshaded areas) [14]. Due to the bulk-current picture, a plateau transition happens, if the one phase takes over from the other and this happens around the half-filled LL. In context with **Figure 8** and Eq. (8), we get the quite simple and universal looking equation $P = \exp[-\Delta N]$, where ΔN is the number of electrons that are either in excess or missing from an exactly half-filled Landau level on a square defined by the period L.

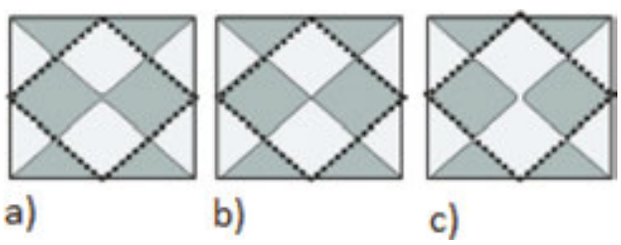

Figure 8. Top view of a complete period L containing a central saddle at (a) Fermi energy slightly above saddle energy, (b) Fermi energy exactly at saddle energy, (c) Fermi energy slightly below saddle energy. The areas filled with electrons are shaded; the unshaded areas are empty.

A major necessary further step is now the introduction of a disorder potential. This is achieved by the superposition of a random potential to the so far regular saddle potentials. That leads to the effect that no longer all nodes behave the same. Looking at the filling factor representation, a random potential also leads to a lateral fluctuation of the local filling factors at the positions of the nodes.

Including an additional long range disorder potential, the saddle energies get nonuniformly distributed and a partly transmission and reflection at the nodes appears only at those locations where the saddle energy stays close to the Fermi energy. This usually happens only for a small fraction of the nodes in the network, like indicated schematically in **Figure 9**. All nodes (saddles) with energy far from the Fermi energy have either full transmission ($T = 1$, $R = 0$) or full reflection ($T = 0$, $R = 1$), depending on whether the Fermi energy is above or below the saddle energy. In this way, the network guides the channels around potential fluctuations and only those nodes at which the saddle energy gets close to the Fermi energy become physically active as tunneling junctions (red arrows in **Figure 9**). In this context, our network, which we

call non-equilibrium network model (NNM) can be understood as a method to approximate arbitrarily shaped magnetic bound states and it also finds the "hot spots" (active saddles of the disordered potential).

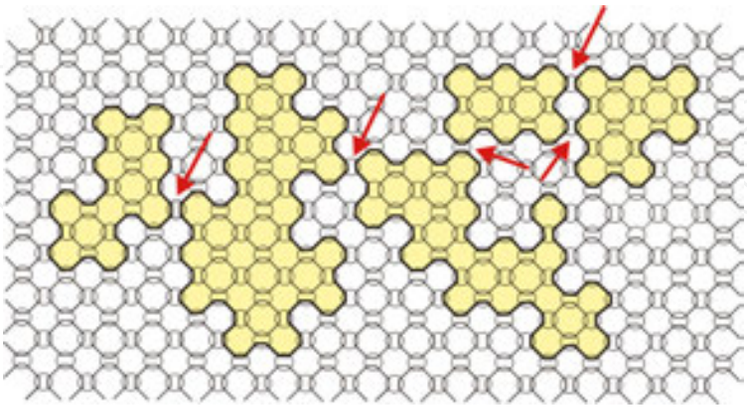

Figure 9. Schematic representation of the effect of a random potential that is superimposed on the regular periodic grid of saddles. The yellow areas indicate regions of saddle potentials below the Fermi energy that lead to higher carrier density and hence local filling factors larger than ν=0.5, while the white areas indicate larger saddle potentials above the Fermi level leading to lower carrier density and hence local filling factors lower than ν=0.5. At the boundaries between these regions we cross the situation of half-filled LLs, where the Fermi energy meets saddles and as discussed already before, while crossing the saddle energy the involved nodes turn by 90°. This can be seen by either following a particular row or column of nodes if we enter or leave the yellow colored area.

The NNM as introduced so far is a standalone model for describing the non-equilibrium transport that means the lateral distribution of the disruption from thermal equilibrium. The physics, how the screened potentials or local filling factors are obtained as input information for the nodes, is not directly addressed by the NNM. There exist different levels for approaching the underlying electron system from semiclassical screening effects that neglect exchange interaction to a full treatment as many-particle system on, for example, the Hartree–Fock level. While for the semiclassical model, the screened electrostatic potential can be used as an input for the network, this might not be sufficient for the Hartree–Fock treatment, because the exchange contribution might dominate over the pure classical electrostatic part of the carrier distribution, and therefore, there is good reason to use the network representation in terms of the local filling factors.

Another very important aspect of our non-equilibrium network model is that it addresses finally only the lateral distribution of the non-equilibrium excitation potentials without explicitly relating to quantities like local currents or local conductivities, which would be in violation of the many-particle physics, because of implying an existence of individual electrons in the system. The currents of the non-equilibrium are not addressed while solving the problem. Only as a post-processing step, the currents are calculated just at the contacts where the system communicates with the outside world. Therefore, our network model is compatible also with the demands of many-particle physics, and it is independent of the type of carriers that show up as quasi-particles just at the contact in a post-processing step. In this post-processing step, the type of carriers become relevant only by the way how the current balance

http://dx.doi.org/10.5772/62926

at the contact has to be done. For electrons, this is the usual quantized conductance times the potential difference. At this point it should be reminded that also for the usual electrically confined one-dimensional channels the quantized conductance $G = 2 \cdot e^2/h$ appears only in context with the presence of metallic contacts. However, there is no reason why the same network model should not be used for fractional channels exactly in the same way, where the only modification would be that the current balance at the contact has to be done for the fractional charges of composite fermions. This is the subject of future work.

5. Implications

Many implications of the various approaches and arguments as given above can be found retrospective already in the literature, and therefore, the next paragraph is devoted to numerous already existing implications. For better readability in the above modeling sections, only some of those citations concerning primary resources are contained. It is also worth to mention that the presentation as it appears above is not the chronological process of a recent development. The chronological process contains many partly independent steps collected over almost 20 years of research that finally have been but together by the time. Therefore, there already exists a huge punch of related literature, in which supporting implications for many of the different features and aspects of our model can be found. In this section, we will address part of this additional background literature for the reader to gather some further insights of different aspects, however, without being able to make a full review that would definitely go beyond the boundaries of this chapter.

Let us start directly with Eq. (8) that is one of the major ingredients of our model. Almost 20 years ago, a similar equation has been found to be necessary in order to meet specific symmetry conditions of quantum Hall measurements [15]. That equation has been applied to a quantum Hall sample as a whole and the typical behavior now turns out to apply also for a single node of our network model. Even without creating a full network, there have been attempts to put together an equivalent circuit for a quantum Hall sample. Each channel pair of the whole sample has been handled like a single node of our network, but only for the channel pair representing the top LL backscattering ($P > 0$) has been assumed. The total sample has been modeled by parallel connection of the suitable number of edge channel pairs [16]. Although there have been strong indications that tunneling may play an important role, the particular shape as an exponential function of P versus filling factor ν at that time was found initially just by symmetry requirements. A similar function had been found also by Shahar et al. [17], who needed it for interpretation of experimental data in context with deviations from scaling theory that the authors have been observing. Their results have been inspiring in the sense that the scaling theory is an important aspect of the QHE, but maybe not directly the driving force for the existence of the QHE. A first version of the network model has been formulated on the basis of local filling factors [18], which in turn is based on a special earlier version for addressing the Hall insulator [19]. The tunneling process was explicitly addressed later when looking for a better way to introduce the disorder potential that was expected to be dominated by the screened electrostatic potential [13]. Using just a semiclassical approach to screening for

modeling and shaping the samples structures has already proven to be sufficient for successfully modeling many features of quantum Hall samples in terms of all geometrical aspects like length and distance between contact arms [20], effects of gate electrodes [21, 22], effects due to the different equilibration lengths [20], effects due to the number of contact arms and non-local effects [23], inhomogeneous magnetic fields [24] and also most complex sample geometries like an anti-Hall bar structure that is embedded in a Hall bar [25–27]. The latter demonstrates the appearance of simultaneous independent Hall effects for the inner and outer boundaries of the same electron system that is supplied in parallel by different independent constant current sources. That example was at the same time a demonstration of the flexibility of our network model in terms of addressing most complex experimental conditions.

But even much earlier, we have found indications of such a unique behavior when coupling quantum channels that carry different electrochemical potentials, which now turn out to look similar like the formulations for our network model. That behavior has been found by investigating magneto-transport in quasi-3D systems that do not show quantum Hall effect. In this context, we have performed magneto-transport experiments and modeling for the so-called wide parabolic quantum wells [28, 29]. These structures are no longer two-dimensional because the sub-band splitting is smaller as compared to the LL splitting, which means that those structures are somehow in the regime between 2D and 3D. Although there have not been observed any quantum Hall plateaus, relations between longitudinal and transverse (Hall) resistance have been found that in a retrospective view also support the relations between the chemical potentials as discussed above. The wide parabolic quantum wells at large filling factors had been created by the Narrow Gap Semiconductor PbTe and instead of quantum Hall plateaus magneto-resistance fluctuations have been found at temperatures below 100 mK and at small current of the order of a few nA. The temperature and current dependence of these fluctuations that also appeared in a so-called non-local contact configuration even at macroscopic sample size [30] indicated the involvement of quantum channels [31]. In this context, the relations between the potentials of channels that meet at non-equilibrium situation seem to be valid also for that regime far from the standard quantum Hall regime in the clean two-dimensional case. That can be seen as a hint that the basic principles addressed in the previous sections seem to be more general and hold also beyond the standard quantum Hall regime. There are also other examples from the literature, in which a behavior similar to that in a single node was found by Haug et al. [32]. However, that was derived just for the special case of a gate initiated scattering experiment in the QHE regime and has not been considered further from a more general point of view. Another interesting connection can be found with the work of Chklovskii et al. [33], where the authors deal with the conductance of the central compressible bulk channel. Such a compressible bulk channel appears in the transition regime between conductance plateaus, while successively depopulating the LLs by either increasing the magnetic field or successively narrowing a channel by spit gates until the density in the center falls below the density of a fully populated LL. Besides the screening properties, which the authors handled as a pure classical electrostatic problem, they use some kind of semi empirical formula in order to translate the electron density in the central compressible bulk stripe into a conductance of that stripe:

http://dx.doi.org/10.5772/62926

$$G = \frac{e^2}{h} \cdot \nu(0) \tag{9}$$

Here, $\nu(0)$ means the filling factor in the center of the compressible bulk channel at $\nu(0) < 1$. This Eq. (9) has been extracted from a paper of Beenakker et al. [34] who deals with edge channel transport in the fractional quantum Hall regime. Equation(9) can be seen as an appropriate approach to give a correct interpolation between conductance steps. At this point, we want to extend the discussion of our model in order to demonstrate that our approach captures the main features of the approach of these authors as well. We make a simplification and use only a single node of our network in order to capture the situation of two opposite channels that merge in the centre of a sample. This situation has been already addressed in Ref. 13 (there in context to **Figure 14**). It can be also understood if considering just a single node like in **Figure 5**. Without backscattering (P = 0), the quantized conductance of the node for transmission from right to left is $G = e^2/h$. This value would be measured only if terminals 2 and 3 of the node are connected together at an ideal metallic contact on the left and terminals 1 and 4 are connected to another ideal metallic contact of the right. If applying a potential difference between those contacts, a current according to that quantized conductance e^2/h would flow. If we now merge the channels in the centre of the nodes, reflection and transmission get equal probability, which means $R = T = 0.5$ and $R/T = 1$. According to Eq. (4), this means that the junction itself represents the universal conduction e^2/h that adds another universal conductance in series to the backscattering free case, which means that now we have connected in series two times the universal conduction which gives in total:

$$G = \frac{e^2}{h} \cdot 0.5$$

This fits exactly Eq. (9) for ν(0) = 0.5, which means a half-filled LL. Obviously, this is also in agreement with Eq. (8), for which the exponent vanishes right at a half-filled LL. The advantage in our case is that we can extend our model to a network in order to capture further details like length, width, and also inhomogeneities of the metallic bulk stripe, while the authors of Ref. [33] have to restrict them self to special cases and assumptions. Another point is that the approach of Chklovskii et al. provides no handle for extending their approach beyond semiclassical treatment of the stripes, and therefore, they neglect many body effects that have been found to play an important role in the quantum Hall regime. Since we consider current transport from a most general point of view and taking into account facts related to many-particle physics, the application of our transport model has no such restriction and can be applied also to a modeling based on many body effects, as will be demonstrated in the next section.

The fact, that there can be found numerous implications for the basic behavior that is represented by the nodes of the network, suggests that there are more general aspects behind that might be interesting also for communities outside the quantum Hall community. That was finally the motivation to propose this chapter as a very fundamental step toward introducing some kind of dynamic in terms of stationary net current flow close to thermal equilibrium while starting from the stationary many-particle ground states. In the final chapter, we present some most recent results for the quantum Hall regime on the basis of a many-particle system by applying the Hartree–Fock approximation for finding the stationary ground state and introducing the presented treatment of non-equilibrium for obtaining the longitudinal and Hall resistances as a function of magnetic field.

6. Recent results

In the previous section, we have presented a selection of examples for implications of our model that can be already found in the literature that give support for the results of our modeling. This is done mainly just by referring to the literature without reproducing the results in detail. Therefore, the reader is advised to refer to the cited literature for further details. In this paragraph, we want to present most recent results by taking into account the many-particle physics up to the Hartree–Fock level including disorder. The particular numerical Hartree–Fock approximation as used here has been outlined in several publications, and therefore, the reader is also advised to look up further details in the given Refs. [35–37]. Here, we will just present the results for two examples.

6.1. Imaging of condensed quantum states

The first example deals with a many-particle system that contains only few electrons that get localized in some model potential and which do not directly contribute to transport. This system is considered as embedded in a conducting environment and the impact of the charge distribution of such a localized state on the tunneling barrier of a nearby quantum point contact (QPC) is taken into account. Such a QPC can be understood as a saddle potential that acts as a charge detector for nearby charge distributions. In this case, the nodes of the network for transport at the QPC are controlled by the local potentials based on Eq. (7). For demonstration, an artificial confining potential ring (see **Figure 10**) has been created and filled with eight electrons. These eight electrons are treated as a many-particle system using the Hartree–Fock method and as shown in **Figure 11** the charge density resembles a periodic structure along the ring that can be understood also as a one-dimensional Wigner crystal. Here, just the main results are presented and for further details please refer to Ref. [38]

The eight confined electrons have been treated as a many-particle system separately from the conducting environment that has been represented by a semiclassical approach based on Eq. (7) of the NNM. The presence of the charge distribution in the ring was taken into account by using the recalculated Hartree potential of the charge distribution in the ring at the potential saddles of the QPCs. The transmission of the QPCs, that have been modeled using the network

http://dx.doi.org/10.5772/62926

model as described above, has been calculated, while a repulsive potential distortion was superimposed at different locations in the ring area. The potential distortion represents the moving tip of a so-called scanning gate microscope [39]. The effect of the tip on the condensed quantum state affects the charge distribution, which affects the nearby saddle potentials that finally modulates any tunneling current in the environment nearby the ring. If a current in the environment of the ring passes those saddles, this current give a response if the SGM-tip hits the charge maxima of the condensed state. If the total sample current is recorded as a function of tip position, the response pattern creates something like an image of the charge distribution of the quantum state.

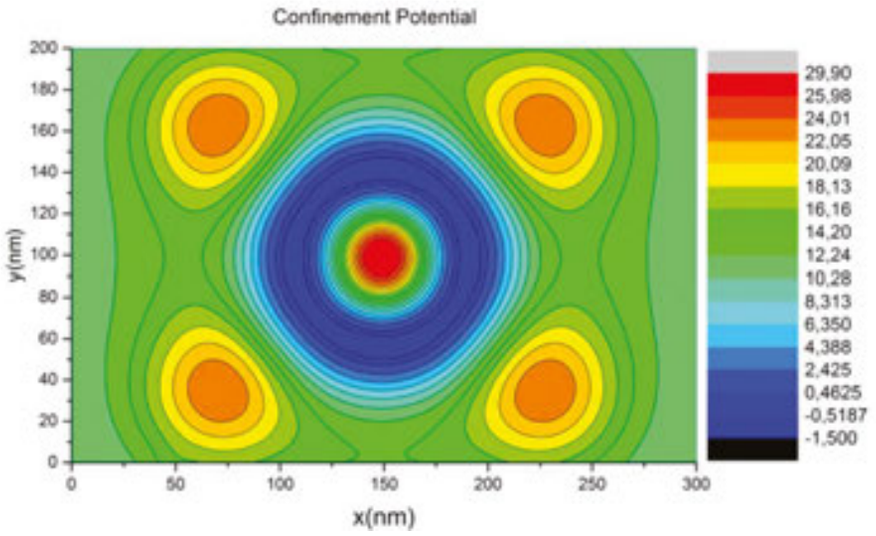

Figure 10. Contour plot of the bare ring-shaped confinement potential with a diameter of about 100 nm and a depth of about 15 meV as compared to the saddle energies of the QPCs.

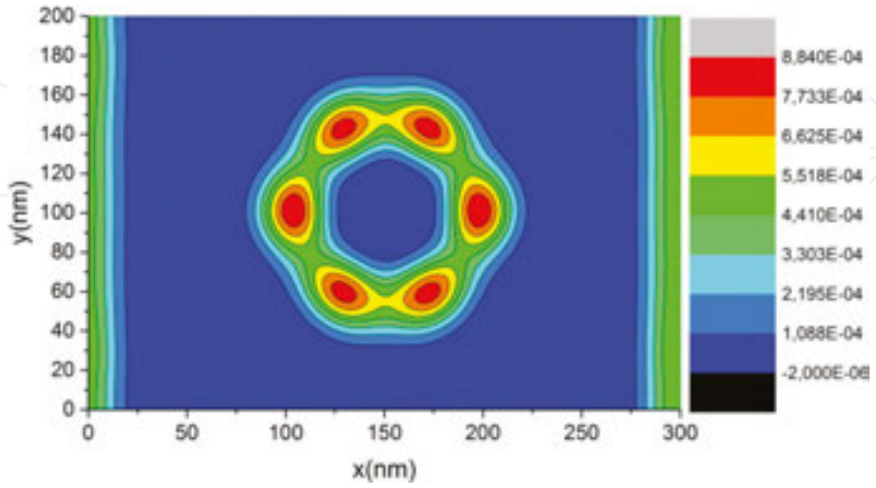

Figure 11. Contour plot of the charge distribution obtained from the Hartree–Fock calculation in multiples of $10^{14}cm^{-2}$ for a magnetic field of B = 2.5 Tesla. In this regime, the electron system appears fully spin polarized.

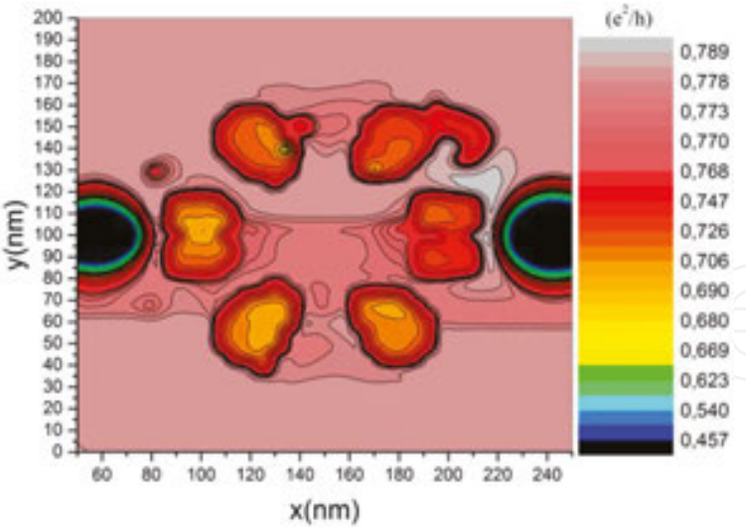

Figure 12. SGM response pattern as a contour plot of the two-point conductance (in multiples of e^2/h) of a nearby QPC in the tunneling regime as a function of SGM tip position. Tip parameters: circular Gaussian shape of repulsive height 1 mV and half-width diameter of 20 nm.

Figure 12 shows the response pattern of the total current that passes the nearby potential saddles and indeed this pattern images the charge distribution in the ring, even though the electrons in the ring are excluded from transport.

It is important to note that this is just a demonstration of the mechanism that transfers information from a decoupled localized many-particle quantum state to a current response of a nearby electron system. A more realistic structure requires a much larger system size of up to several microns length that so far is out of reach for our simulation capabilities. Therefore, in our example, the space beyond the QPC's that carries the environmental current can be understood to be folded back to the same area of the localized states and thus is used twice as some kind of second layer in the model, but assuming that this current bypasses the localized states. The necessary extensions of the model are the subject of ongoing work which needs also to acquire more computing power.

Anyway, this example demonstrates the basic mechanism that allows the SGM-method to create images of charge distribution from condensed quantum states and serves at the same time as an example for the application of the network model for transport where the driving force is coulomb interaction that can be addressed by using Eq. (7) for controlling the nodes of the network.

6.2. Quantum transport at large filling factors

The previous example for a system of just few electrons is far from a fully filled Landau level, and the interaction with the environment was still just coulomb interaction that can be handled with the network model on the basis of Eq. (7) as demonstrated. Now, we turn to the extreme opposite regime of many electrons that fill up several LLs. That means that now we have of the order of 500 electrons in the system instead of eight electrons that is addressed by the

http://dx.doi.org/10.5772/62926

Hartree–Fock model. We use a random potential at an average carrier density of 2×10^{11} cm^{-2}. Because of the many-particle physics at higher-filled LLs, we have to expect that the usage of the Hartree potential for the network will be insufficient because we expect a significant impact from the exchange interaction. In this case, the better representation of the electronic system for the NNM is therefore the local filling factor that is controlled by both the Hartree and the exchange interaction. Once more we want to bring to attention that also Beenakker [34] had found the local filling factor to be relevant for the transport behavior also in the fractional quantum Hall effect, where many-particle physics plays the dominant role. We have compared both methods and plotted the results on top of each other. Exchange-driven effects are lost if using just Eq (7) that also means that enhanced spin splitting is lost because that results from the exchange-driven enhancement of the g-factor. In order to get the right position of the peaks in QHE, one has to introduce the exchange-enhanced g-factor into the NNM, while no such adjustments are needed if using the filling factor version based on Eq. (8). By choice of using Eq. (7) or (8) for the simulation and comparison with experiment, we have a tool to distinguish between effects that are either strongly affected by exchange interaction or not. From our simulations, we get the strong indication that exchange effects are dominating almost all transport regimes that involve more than a single-filled LL even at moderate magnetic fields between B = 1–2 Tesla. That has a significant impact on screening effects that turn out to be strongly reduced as compared to semiclassical modeling as based on, for example, a Thomas-Fermi approach. Investigations concerning the screening properties in context with many-particle physics are in progress.

In the following, we present an example for the simulation of QHE measurements of a disordered sample. The sample is of mesoscopic size of 600 nm length and 400 nm width. We used two degrees of disorder and compare also the different calculation methods, the full many-particle approach in combination with the filling factor version of the NNM as well as the Hartree version.

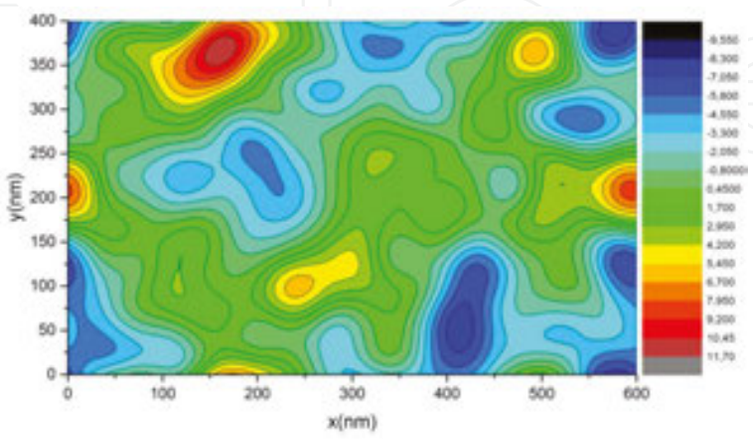

Figure 13. Disorder potential for the case of strong disorder as used for the HF simulation of the bulk region. The colors represent the potential in mV as given in the color map.

Figure 13 shows the bulk potential distribution for the case of strong disorder as used for the Hartree–Fock calculation of the bulk region. Alternatively also a low disorder potential was used that makes use of the same random distribution of Gaussian peaks in order to produce the random potential, but the Gaussians are just half of amplitude and half of width that ends up in a weaker disorder potential. In all cases, an average fixed carrier density of 2×10^{11} cm^{-2} has been used, that results in 480 electrons in the sample area, that get distributed.

The lateral carrier distribution obtained from the Hartree–Fock calculation is shown in **Figures 14** and **15** which show the carrier distributions for spin 1 and spin 2 separately. This is important since it turns out that the many-particle system avoids as good as possible to have partly filled spin 1 and spin 2 LLs at the same time. The calculation was done at magnetic field B = 2.3 Tesla that means a total filling factor close to $\nu = 3.5$. This means automatically that the higher second spin 1 LL remains partly filled, while the lower second spin 2 LL is fully occupied. As can be seen in **Figure 14**, this average filling factor of $\nu = 1.5$ of the spin 1 LLs is achieved by creating areas that are close to filling factor $\nu = 2$ in red and filling factor $\nu = 1$ in blue. That regions are separated by green stripes around filling factor $\nu = 1.5$. An indicated enhanced occurrence of filling factors close to of $\nu = 1.5$ is the subject of ongoing investigations. According to Eq. (8) these green-colored stripes will create stripes of good transmission of the excitation potential in the network model and represent at the same time also the so-called compressible stripes, while the other regions remain insulating. Looking at **Figure 15** for the spin 2 electrons, one can see that the dominating part of the sample area remains close to filling factor $\nu = 2$ which therefore do not contribute to transport that also will have only a weak contribution to screening.

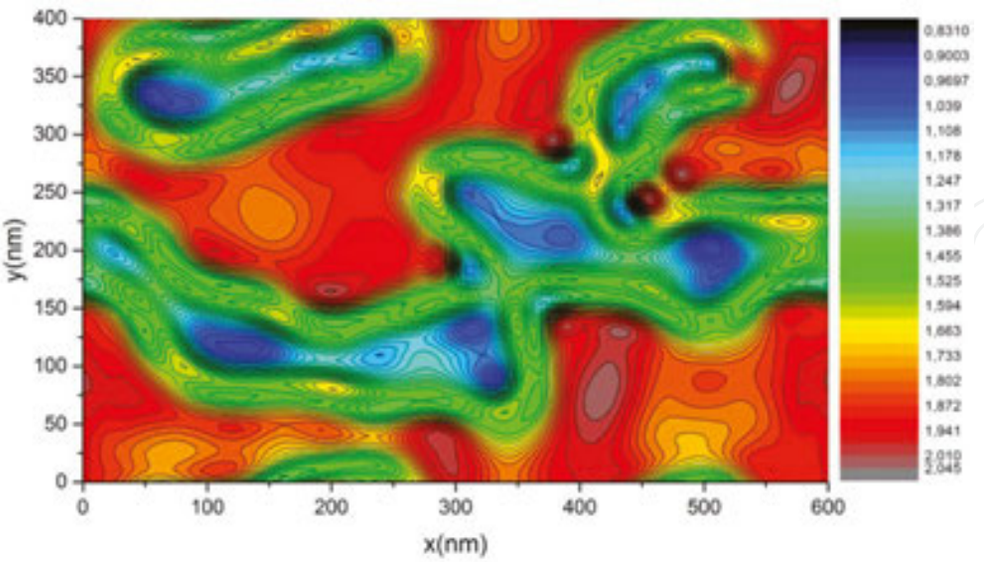

Figure 14. Lateral carrier distribution of the spin 1 electrons, mapped on the filling factor scale. The color mapping ranges over three colors from blue to green to yellow that spans a filling range from about $\nu = 1$ to $\nu = 2$, which means that green appears around filling factor $\nu = 1.5$.

http://dx.doi.org/10.5772/62926

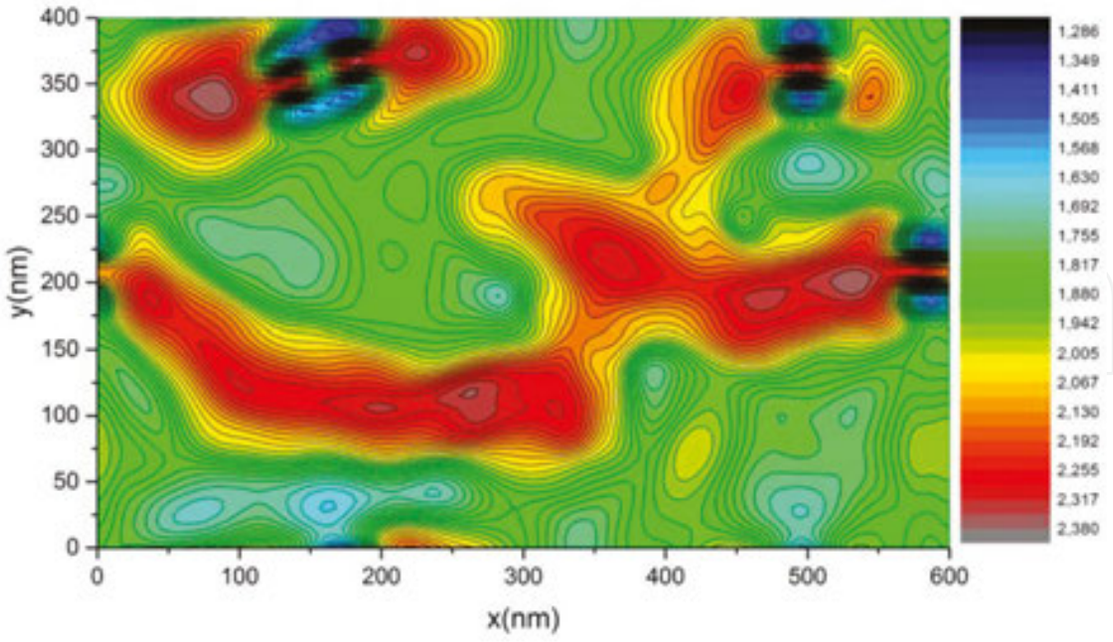

Figure 15. Lateral carrier distribution of the spin 2 electrons, mapped on the filling factor scale. The color mapping ranges over three colors from blue to green to yellow that spans a filling range from about $\nu = 1.5$ to $\nu = 2.3$, which means that green appears close filling factor $\nu = 2$.

The whole calculation has been repeated for different magnetic fields, and the network model has been used to solve the lateral distribution of the excitation potential. For this purpose, the non-equilibrium potential has been set to different fixed values at the supposed current contacts on the left and right boundaries.

In **Figure 16**, there is shown the solution for the lateral distribution of the excitation potential for the same situation like in **Figure 14**. By comparing with **Figure 14**, the transmitting stripes that evolve in the network follow the green stripes. The color represents the potentials that those stripes pick up at the boundaries they are coming from and they may mix up a locations where channels of different excitation potentials meet. By comparing with **Figure 13**, one can see that those stripes follow just roughly the contours of the disorder potential, but deviate from the details. This is a clear indication that besides the Hartree contribution also the exchange interaction is important. After finding the lateral distribution of the excitation potential as shown in **Figure 16**, only directly at the current contacts along sides 1 and 2, the currents are calculated by using Eq. (2) for each channel pair that is arriving at each point of the metallic contacts. Voltage probes have been created at locations 3–6 at the boundaries by just placing a metallic contact, but keeping the potential numerically floating, which means that no current is extracted or injected at those locations. A Hall voltage can be obtained, for example, by taking the difference of the excitation potentials between contacts 3 and 5 or 4 and 6. If dividing by the obtained sample current, we get the Hall resistance that is plotted as a function of the magnetic field. The same can be done for the longitudinal resistance by taking first the potential differences between contacts 3 and 4 or 5 and 6 and dividing by the total current.

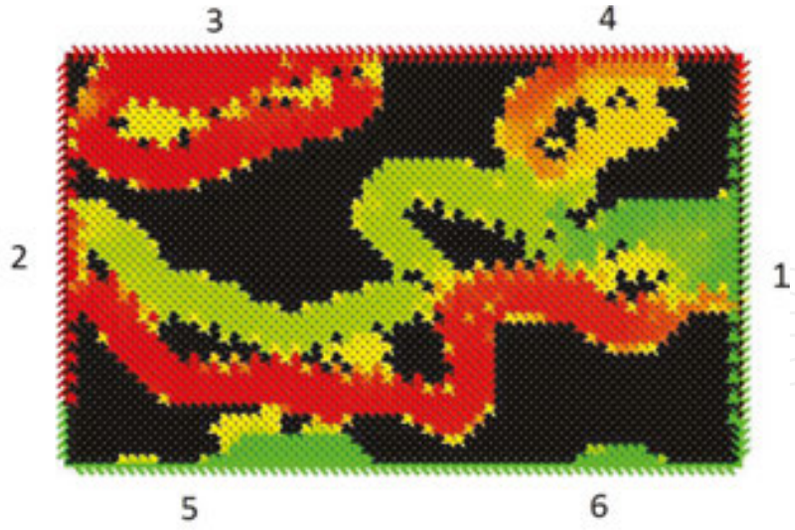

Figure 16. Screenshot of the NNM showing the lateral distribution of the injection potential in the network model. The high potential appears in red and is injected from the left, and the low potential appears in green and is injected from the right. The chirality of the edge channels appears as clockwise. Expect the top spin1 LL, all lower LLs create narrow channels at the network boundaries that experience no backscattering.

In this way, the simulation follows the same procedure like any real experiment that measures voltages and currents and only then the values are translated into resistances, without calculating a total resistance or conductance in terms of butting together elements of any kind of equivalent circuit. In this way, we avoid to use any quantities that might be related to local behavior in terms of conductance or local Ohm's law for the electron system and thus consequently avoid any steps that could be used to attribute single electrons to particular locations or areas of the sample. Constant colour of the stripes in **Figure 16** indicates that there is no current flow within those stripes because of the missing gradient of the chemical potential. The current therefore has to be attributed to the mostly dark regions between stripes of different potential. The current path within these regions remains unknown, like demanded by a quantum system. If stripes of different potential meet the appearing potential gradient (crossing over the yellow colour) between them indicates dissipation in this region. Sometimes numerical noise can also lead to yellow colour in usually de-coupled (black) regions, which, however, does not harm the total current balance.

Figure 17 shows the magnetic field-dependent two-point conductance for strong and low disorder potential and also for the two different methods of incorporating the Hartree–Fock solution into the NNM. Using just the Hartree part of screening of the random potential on the basis of Eq. (7), we have the possibility of manually taking into account exchange-enhanced spin splitting or not. When neglecting the enhanced spin splitting only the even conductance plateaus appear (dashed blue). If introducing the enhanced g-factor manually all plateaus appear correctly also in the Hartree version (red). However, the transition regime looks different if looking at details. Especially, the $\nu = 5$ plateau of the Hartree version (red color) is almost wiped out because of a strong overlap of the spin split $\nu = 5$ LL (see also below). The strongest deviations in the transition regime are between the case of strong (pink color) and

http://dx.doi.org/10.5772/62926

weak disorder (green color), which is not really surprising. For strong disorder, there appear additional overshoots and dips, which result from the fact, that the strong disorder for this small sample dimensions acts already as an inhomogeneity.

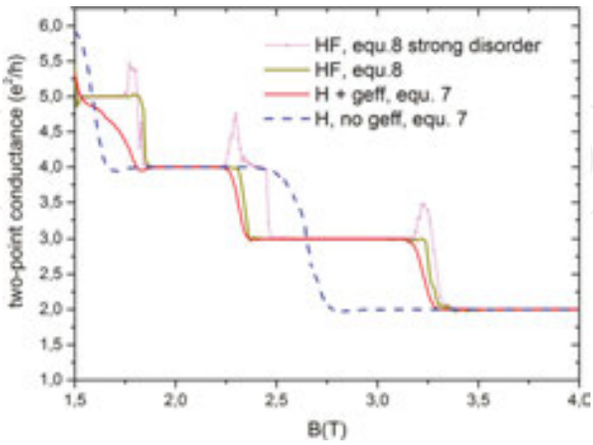

Figure 17. Total sample current mapped out as two-point conductance as a function of the magnetic field. The simulation was done for the structure shown in Figure 13 for the shown strong disorder potential and the not shown weaker disorder potential. HF means that the full Hartree–Fock contribution has been used in the NNM by using the local filling factor on the basis of Eq. (8); H means that the full Hartree–Fock carrier distribution has been obtained as well, but from that only the Hartree potential has been recalculated in order to get its contribution to screening of the random potential and Eq. (7) has been used in the NNM. If using just the Hartree part of screening on the basis of Eq. (7), the LLs have to be calculated separately on the basis of a semiclassical model directly in the NNM, which also requires to use the g-factor the for spin splitting as a semi empirical parameter; the label geff means that a semi empirical enhanced g-factor of geff = 14 has been used, while no geff means that enhanced spin splitting has been neglected.

If extracting potential differences between Hall voltage probes and calculating the Hall resistances for the same cases as in **Figure 17** as a function of magnetic field, we obtain **Figure 18**.

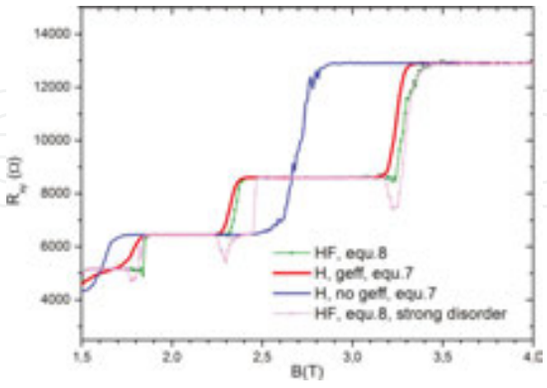

Figure 18. Hall resistance for the same parameters as described in Figure 17.

The Hall plateau values for all cases are of course the same, also the plateau transitions appear almost at the same magnetic fields, just the transition itself is different for the different calculations. An exception is again the non-spin split case (blue) where only the even Hall

plateaus appear. The slight fluctuations in the transition regime comes from the fact that also the Hartree part of the Hartree–Fock solution fluctuates with changing magnetic field, and this is communicated to the NNM as well. When using the enhanced g-factor in the higher magnetic field regime (red), the agreement between the two versions is quite good. Only at low magnetic fields, there is again a strong deviation between the Hartree and the HF version because the semiclassical representation of the LLs in the Hartree version of the NNM overestimates the LL overlap between different spins. This results in a wiped out $\nu = 5$ plateau of red curve. But we know that the Hartree–Fock solution tries to avoid different partly filled spin LLs at the same time, and therefore, the $\nu = 5$ plateau of the HF versions is still well developed (green). For the strong disordered and almost inhomogeneous sample, we get strong fluctuations and over shoots in the plateau transitions (pink)

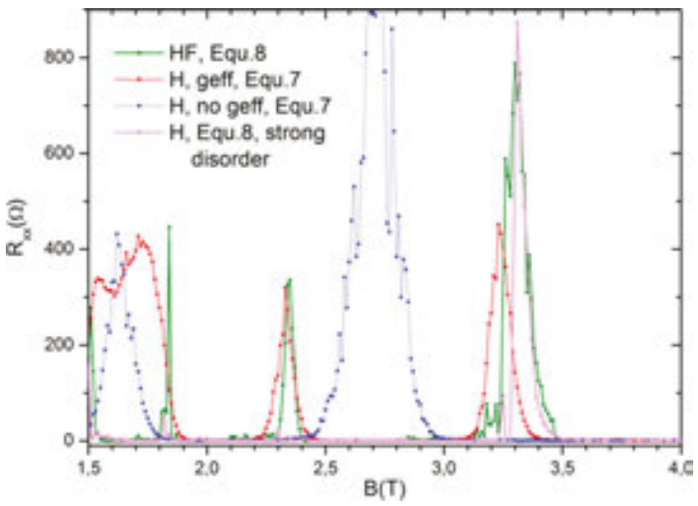

Figure 19. Longitudinal resistance versus magnetic field for the same cases as explained in context with Figure 17.

Figure 19 finally shows the longitudinal resistance for the different cases. The overall shape is covered with strong magneto-resistance fluctuations for all cases, as one expects from QH samples of mesoscopic size. The peak positions of the Hartree version with correctly set enhanced g-factor (red) matches quite well the HF-version (green), again except at fields below B = 2 Tesla. Here, the Hartree version (red) produces a strongly overlapping double peak that results from the overlapping spin 1 and spin 2 levels of the third LL. Exchange interaction counteracts this overlap, and therefore, there appear two separated sharp peaks for the HF version (green), one at B = 1.5 Tesla that corresponds to $\nu = 5.5$ and the other at 1.85 Tesla that corresponds to $\nu = 4.5$. For strong disorder, the R_{xx} peaks (pink) are almost missing in the field range below 3 Tesla. That can be understood by the fact, that the strong disorder produces already an inhomogeneity that can lead to the fact, that not all edge channels reach also the voltage probes at the boundaries, as e.g. can be seen in **Figure 16**. This results in the fact that any dissipation that is generated by the two inner stripes is not monitored by the contacts at the boundaries, and therefore, the associated R_{xx} peaks are missing. The blue dashed curve again represents the Hartree version without enhanced spin splitting, which means that the R_{xx} peaks appear at odd filling factors $\nu = 5$ and $\nu = 3$, where both overlapping spin 1 and spin

http://dx.doi.org/10.5772/62926

2 levels of LL 3 and LL2 are taken into account as half filled, which is not the case in the HF solution because of the enhanced spin splitting.

7. Summary

Based on a fundamental discussion of the many-particle aspects of the electron system, we have presented a modified way to look at the many-particle electron system in terms of a single-particle picture that considers channels for current flow from a more general point of view. While quantum channels like the edge channels in the QHE regime can be identified as locations on the sample area where current exchange for transport experiments is possible, one must not attribute any current flow exclusively to those channels like for classical wires; instead, the whole electron system is understood to carry the sample current, while it is not possible to track individual electrons through the electronic system. Instead of directly addressing current flow, we describe the lateral transmission of the experimentally introduced non-equilibrium electrochemical potentials between such channels on the bases a network approach. This network is used to find a solution for the lateral distribution of the injected non-equilibrium without needing to consider explicitly current flow or local conductances. Conductances come into play only in context with experiments when extracting electrons just directly at contacts by relating the applied non-equilibrium potentials and the resulting flow of electrons through these contacts. Only the lateral distribution of the non-equilibrium potentials is found by our network model on the basis of an iterative procedure, and currents are only obtained as a post-processing step just directly at the current contacts where the electrons are extracted like also in real experiments! This makes our transport model also applicable for systems that forbid the way of thinking in terms of single electrons moving through the electron system, like this is the case in many-particle systems. This has been demonstrated by applying our transport model to the many-particle electron system for which realistic results have been achieved by simulating quantum Hall measurements for disordered samples of mesoscopic size. This makes our network model also applicable for the fractional quantum hall regime, which is the topic of future work.

Acknowledgements

JO acknowledges support from Austrian Science Foundation FWF Project P19353-N16. JO thanks R. Römer for his important cooperation in context with implementing the Hartree-Fock method for the non-equilibrium network model, as well as for substantial discussions and providing access to computing facilities via partial support from EPSRC Grant EP/J003476/1 and provision of computing resources through the MidPlus Regional HPC Centre Warwick UK (EP/K000128/1).

Author details

Josef Oswald

Address all correspondence to: josef.oswald@unileoben.ac.at

Institute of Physics, Montanuniversität Leoben, Leoben, Austria

References

[1] Vonklitzing, K., Dorda, G., Pepper, M. New method for high-accuracy determination of the fine-structure constant based on quantized Hall resistance. Physical Review Letters. 1980; 45(6): 494–497.

[2] Huckestein, B. Scaling theory of the integer quantum Hall-effect. Reviews of Modern Physics. 1995;67(2): 357–396. doi:10.1103/RevModPhys.67.357

[3] Hohls, F., Zeitler, U., Haug, R. J. Hopping conductivity in the quantum Hall effect: Revival of universal scaling. Physical Review Letters. 2002; 88(3): 036802. doi:10.1103/PhysRevB.88.036802

[4] Engel, L. W., Shahar, D., Kurdak, C., Tsui, D. C. Microwave frequency-dependence of integer quantum Hall-effect—Evidence for finite-frequency scaling. Physical Review Letters. 1993; 71(16): 2638–2641. doi:10.1103/PhysRevLett.71.2638

[5] Kubo, R. Statistical-mechanical theory of irreversible processes. 1. General theory and simple applications to magnetic and conduction problems. Journal of the Physical Society of Japan. 1957; 12(6): 570–586. doi:10.1143/jpsj.12.570

[6] Buttiker, M. Absence of backscattering in the quantum Hall-effect in multiprobe conductors. Physical Review B. 1988; 38(14): 9375–9389.

[7] Roothaan, C. C. J. New developments in molecular orbital theory. Reviews of Modern Physics. 1951; 23(2): 69–89. doi:10.1103/RevModPhys.23.69

[8] Oswald J. On the Landauer formula and the edge channel picture of the integer quantum Hall effect. In: Miura, N., Ando, T., editors. Proceedings of the 25th International Conference on the Physics of Semiconductors, Pts I and Ii; Sep 17–22, 2000; Osaka, Japan. Springer Proceedings in Physics; 2001. pp. 977–978.

[9] Sohrmann, C., Oswald, J., Roemer, R. A. Quantum percolation in the quantum Hall regime. Quantum and Semi-Classical Percolation and Breakdown in Disordered Solids. 2009; 762: 163–193. doi:10.1007/978-3-540-85428-9_6

[10] Hashimoto, K., Sohrmann, C., Wiebe, J., Inaoka, T., Meier, F., Hirayama, Y., Roemer, R. A., Wiesendanger, R., Morgenstern, M. Quantum Hall transition in real space: From

localized to extended states. Physical Review Letters. 2008; 101(25): 256802. doi:10.1103/PhysRevLett.101.256802

[11] Chalker, J. T., Coddington, P. D. Percolation, quantum tunnelling and the integer Hall-effect. Journal of Physics C: Solid State Physics. 1988; 21(14): 2665–2679. doi: 10.1088/0022-3719/21/14/008

[12] Kramer, B., Kettemann, S., Ohtsuki, T. Localization in the quantum Hall regime. Physica E-Low-Dimensional Systems & Nanostructures. 2003; 20(1–2): 172–187. doi: 10.1016/j.physe.2003.09.034

[13] Oswald, J., Oswald, M. Circuit type simulations of magneto-transport in the quantum Hall effect regime. Journal of Physics-Condensed Matter.2006; 18(7): R101–R138. 18(7): R101–R138. doi:10.1088/0953-8984/18/7/r01

[14] Ruzin, I., Feng, S. C. Universal relation between longitudinal and transverse conductivities in quantum Hall-effect. Physical Review Letters. 1995; 74(1): 154–157

[15] Oswald, J., Span, G., Kuchar, F. Universality in the crossover between edge-channel and bulk transport in the quantum Hall regime. Physical Review B. 1998; 58(23): 15401–15404

[16] Oswald J. A new model for the transport regime of the integer quantum Hall effect: The role of hulk transport in the edge channel picture. Physica E. 1998; 3(1–3): 30–37

[17] Shahar, D., Hilke, M., Li, C. C., Tsui, D. C., Sondhi, S. L., Cunningham, J. E., Razeghi, M. A new transport regime in the quantum Hall effect. Solid State Communications. 1998; 107(1): 19–23

[18] Oswald, J., Homer, A. A new network model for the integer quantum Hall effect. Physica E-Low-Dimensional Systems & Nanostructures. 2001; 11(4): 310–322

[19] Oswald, J., Homer, A., Ganitzer, P. A network model for the Hall insulator. Microelectronic Engineering. 1999; 47(1–4); 31–33

[20] Oswald J. The role of edge channel equilibration for the R_{xx}—Peak height of the integer quantum Hall effect. In: 15th International Conference on High Magnetic Fields in Semiconductor Physics, SEMIMAG, 5–9 Aug, 2002, Oxford, UK, CD-ROM

[21] Oswald, J., Uiberacker, C. Gate controlled separation of edge and bulk current transport in the quantum Hall effect regime. Journal of Low Temperature Physics. 2010; 159(1–2): 180–183

[22] Oswald, J., Uiberacker, C. Gate Controlled Narrowing of the Quantum Hall Effect Plateau Transitions. In: Goll, G., Lohneysen, H. V., Loidl, A., Pruschke, T., Richter, M., Schultz, L., Surgers, C., Wosnitza, J., editors. International Conference on Magnetism (ICM 2009), Jul 26–31, 2009, Karlsruhe, GERMANY. Journal of Physics Conference Series. 2010; 200. doi:10.1088/1742-6596/200/1/012153

[23] Oswald, J., Uiberacker, C., Stecher, C. A Numerical Study of Non-local Magneto Transport Effects in Quantum Hall Device Structures. In: Muraki, K., Takeyama, S.,

editors. Horiba International Conference: The 19th International Conference on the Application of High Magnetic Fields in Semiconductor Physics and Nanotechnology. Journal of Physics Conference Series. 2011; 334. doi:10.1088/1742-6596/334/1/012020

[24] Oswald, J., Uiberacker, C. A Numerical Study of Magneto Transport in 2D Electronic Systems in the Presence of Non-Uniform Magnetic Fields. In: Ihm, J., Cheong, H., editors. Physics of Semiconductors: 30th International Conference on the Physics of Semiconductors; Jul 25–30, 2010, Seoul, South Korea. AIP Conference Proceedings 1399; 2011.

[25] Oswald, M., Oswald, J., Mani, R. G. Voltage and current distribution in a doubly connected two-dimensional quantum Hall system. Physical Review B. 2005; 72(3): 035334

[26] Oswald, J., Oswald, M. Magnetotransport in a doubly connected two-dimensional quantum Hall system in the low magnetic field regime. Physical Review B. 2006; 74(15): 153315

[27] Uiberacker, C., Stecher, C., Oswald, J. Microscopic details of the integer quantum Hall effect in an anti-Hall bar. Physical Review B. 2012; 86(4): 045304

[28] Oswald, J., Span, G. Novel non-local behaviour of quasi-3D wide quantum wells. Semiconductor Science and Technology. 1997; 12(3): 0268–1242

[29] Oswald, J., Span, G., Homer, A., Heigl, G., Ganitzer, P., Maude, D. K., Portal, J. C. Anomalous magnetotransport in wide quantum wells. Solid State Communications. 1997; 102(5): 391–395. doi:10.1016/s0038-1098(97)00017-3

[30] Oswald, J., Heigl, G., Span, G., Homer, A., Ganitzer, P., Maude, D. K., Portal, J. C. Conductance fluctuations in PbTe wide parabolic quantum wells. Physica B. 1996; 227(1–4): 360–362. doi:10.1016/0921-4526(96)00442-5

[31] Homer, A., Ganitzer, P., Span, G., Oswald, J. A novel transport model for the metal-to-insulator transition in quasi-three-dimensional wide quantum wells. Superlattices and Microstructures. 1999; 25(1–2): 191–196. doi:10.1006/spmi.1998.0636

[32] Haug, R. J., Kucera, J., Streda, P., Vonklitzing, K. Scattering experiments in two-dimensional systems in the presence of quantizing magnetic-fields. Physical Review B. 1989; 39(15): 10892–10900. doi:10.1103/PhysRevB.39.10892

[33] Chklovskii, D. B., Matveev, K. A., Shklovskii, B. I. Ballistic conductance of interacting electrons in the quantum Hall regime. Physical Review B. 1993; 47(19): 12605–12617. doi:10.1103/PhysRevB.47.12605

[34] Beenakker, C. W. J. Edge channels for the fractional quantum Hall-effect. Physical Review Letters. 1990; 64(2): 216–219. doi:10.1103/PhysRevLett.64.216

[35] Roemer, R. A., Sohrmann, C. Hartree-Fock interactions in the integer quantum Hall effect. Physica Status Solidi B: Basic Solid State Physics. 2008; 245(2): 336–343. doi: 10.1002/pssb.200743321

[36] Sohrmann, C., Roemer, R. A. Kubo conductivity in the IQHE regime within Hartree-Fock. Physica Status Solidi C: Current Topics in Solid State Physics. 2008; 5(3): 842–847. doi:10.1002/pssc.200777586

[37] Sohrmann, C., Roemer, R. A. Compressibility stripes for mesoscopic quantum Hall samples. New Journal of Physics. 2007; 9. doi:10.1088/1367-2630/9/4/097

[38] Oswald J., Römer R. A. Imaging of condensed quantum states in the quantum Hall effect regime. Physics Procedia. 2015; 75: 314–325. doi:10.1016/j.phpro.2015.12.038

[39] Sellier, H., Hackens, B., Pala, M. G., Martins, F., Baltazar, S., Wallart, X., Desplanque, L., Bayot, V., Huant, S. On the imaging of electron transport in semiconductor quantum structures by scanning-gate microscopy: Successes and limitations. Semiconductor Science and Technology. 2011; 26(6): 064008. doi:10.1088/0268-1242/26/6/064008

IntechOpen